



Solvothermal synthesis and characterization studies of Nickel Oxide Nanoparticles

P. Ajith¹, M. Sappani Muthu¹, J. Agnes¹, D. Prem Anand^{1*}

1. Materials Research Centre, Dept. Of Physics, St. Xavier's College (Autonomous), Palayamkottai-627002, Tamilnadu, India.

Affiliated to Manonmaniam Sundaranar University, Abishekapatti-627012, Tirunelveli, Tamilnadu, India.

1. Materials Research Centre, Dept. Of Physics, St. Xavier's College (Autonomous), Palayamkottai-627002, Tamilnadu, India.*

Abstract

Nickel Oxide Nanoparticles (NiO) were synthesized through solvothermal process. The properties of as prepared NiO nanoparticles were confirmed by analytical techniques such as XRD, FTIR and SEM studies. From XRD analysis, it is clear that the observed peaks revealed that the particle corresponds to face centred cubic structure. The various functional groups in NiO nanoparticles were ascertained by FTIR analysis. Morphological studies were estimated using SEM analysis.

1. Introduction

In the recent past, Nickel Oxide (NiO) has been received considerable attention due to their outstanding electrical, magnetic and catalytic properties, electrochromic films, fuel cells electrodes, gas sensors, battery cathodes, magnetic materials, photovoltaic devices, electrochemical super capacitors, smart windows and dye sensitized photocathodes [1-14]. Additionally Nickel Oxide is a p-type wide band gap (3.6 to 4.9 eV) semiconductor with high electrical and chemical stability [15]. These unique properties and a vast variety of applications of Nickel Oxide make viable and cost effective surface available for hydrogen storage, photo catalytic degradation of organic dyes and antimicrobial activity [15-22]. So far various synthesis methods such as electrochemical reduction, chemical reduction, solgel have been reported to synthesize NiO nanoparticles. Of late, the solvothermal synthesis has been proposed as a cost effective, nontoxic and environmental friendly method. The characterization study of as prepared NiO nanoparticles were characterized by XRD, FTIR and SEM analyses.

2. Experimental

2.1 Chemicals and reagents

All chemicals used in this experiment were of analytical grade. The chemicals used in the synthesis were Nickel Nitrate ($\text{Ni}(\text{NO}_3)_2 \cdot 6\text{H}_2\text{O}$), citric acid and ethylene glycol. All the solutions were prepared in deionized water.

2.2 Synthesis of NiO –Nanoparticles

Nickel nitrate solution was mixed in deionized water. In another beaker citric acid solution was prepared in double distilled water. These two mixtures were added continuously and stirred for an hour with a stirring rate of 300 rpm. Ethylene glycol was then mixed into drop wise with continuous stirring for five hours. The resultant precipitate was then obtained and it was washed with double distilled water. The obtained precipitate was undergone for a heat treatment at 400⁰ c for two hours in a furnace. Finally green coloured NiO nanoparticles were obtained. The flow chart for the synthesis of NiO nanoparticles is shown in the Fig 1. The reaction process of as prepared NiO nanoparticles are given in three stages as shown below.

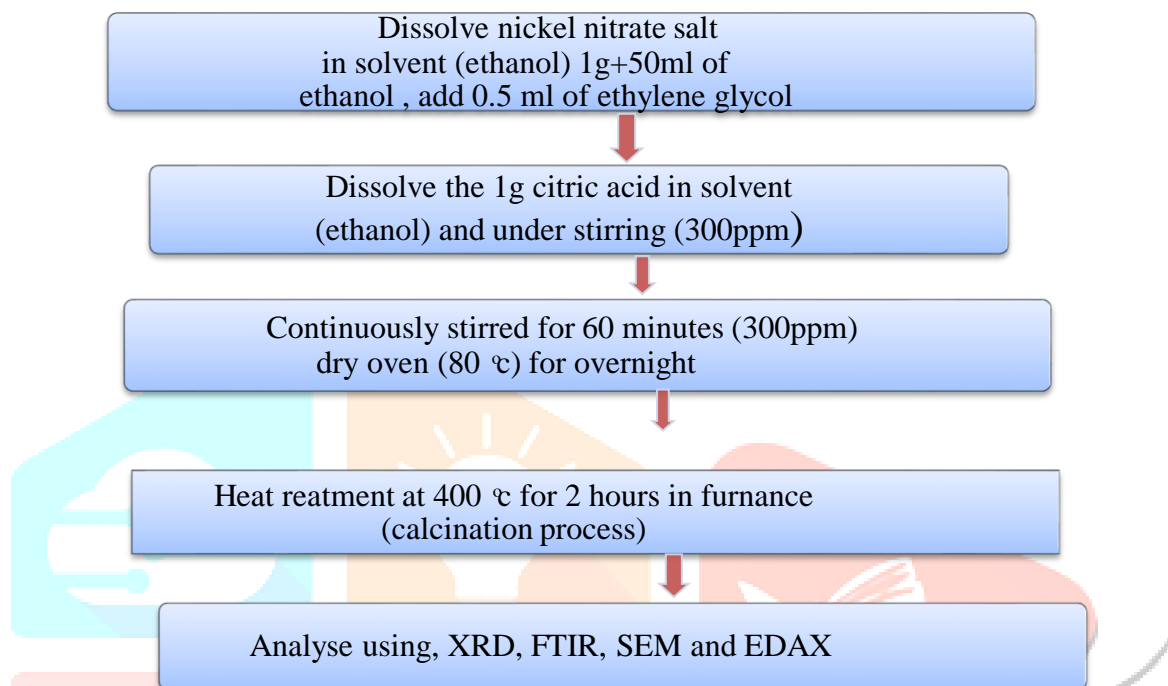


Fig 1. Flow chart for the preparation of as prepared NiO nanoparticles

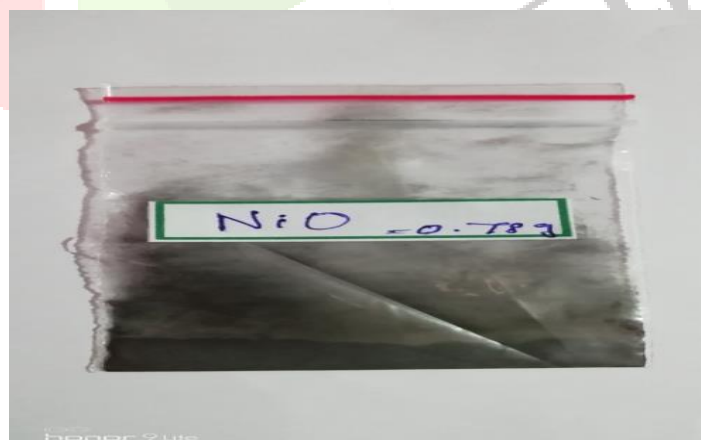


Fig 2. Photograph of as prepared NiO nanoparticles

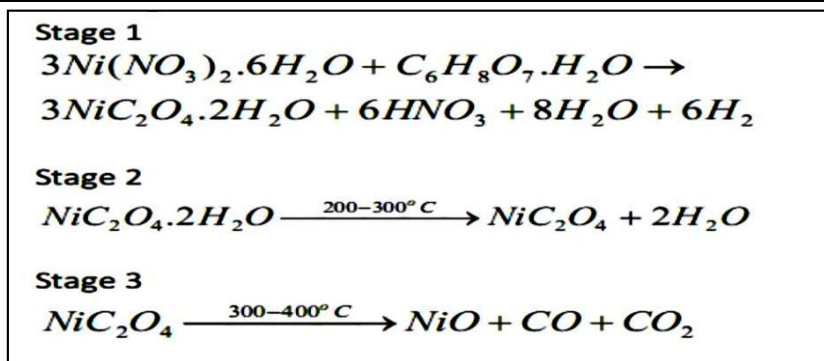


Fig 3. Reaction scheme for as prepared NiO nanoparticles

2.3 Characterization techniques

X-Ray diffraction patterns were taken by a means of X ray diffractometer model Dmax-2500 (The Netherlands) X ray source was $CuK\alpha$ with 1.541 nm wavelength and 30 mA with a scanning speed in 2θ of 4 min^{-1} . FTIR analysis was carried out using on a Perkin – Elmer spectrometer at a spectral resolution of 4 cm^{-1} in kBr pellet. EDAX spectrum was obtained on EDAX GENESIS 4000 equipment at an accelerating voltage of 25 keV. The crystallite sizes of Nickel Oxide were estimated using the Debye – scherrer equation. The surface morphology of NiO nanoparticles were observed by a means of scanning electron microscope (Philips XL30 Microscope) operated at 10 kv. For a UV absorption spectra the samples were dissolved in glycerine with an help of magnetic stirrer for an hour at room temperature and then it was examined by UV-Visible spectrometer.

3. Characterization studies

3.1 XRD analysis

The XRD spectrum of as prepared NiO nanoparticles is shown in the Figure 4

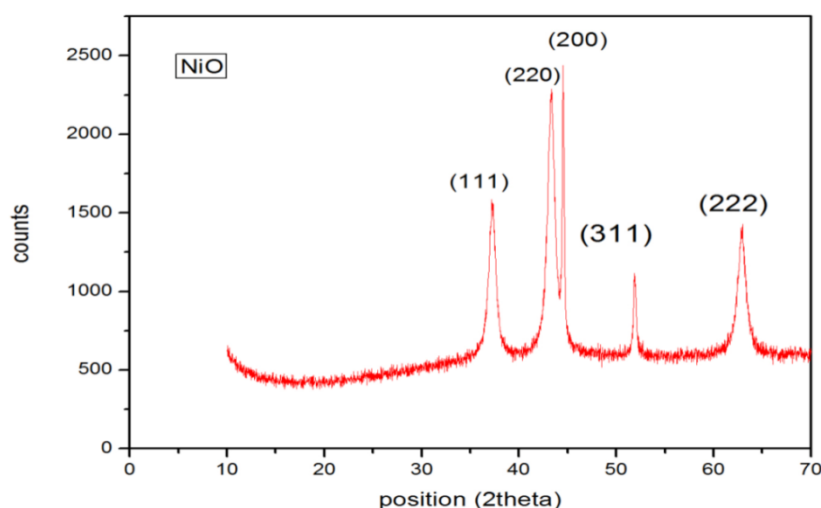


Figure 4. XRD spectrum of as prepared NiO nanoparticles

The Figure depicts the calcination of $400^\circ C$ was in need to completely oxidize metallic Nickel. Accordingly, the formation of Nickel and NiO nanoparticles and their structural features are dependent on the calcination temperature. With increasing calcination temperature, the intensity of the diffraction peaks of NiO increased and the degree of the crystallinity is improved. Before calcination, the samples was in amorphous phase and so NiO phase was observed. After calcination crystalline phase shows a cubic structure, in which all diffraction lines of NiO were indexed to an ordered structure (JCSd 98-009-6203). At the crystalline phase, all diffraction peaks at (111), (220),(200),(311),and (222) were observed. In the amorphous phase, no

significant change in the Nickel phase occurred. Thus no NiO phase existed. The crystalline phase existed after calcination, exhibiting that the metallic Nickel nanoparticles were readily oxidised by NiO nanoparticles. The XRD pattern of all randomly oriented powder samples were recorded in the 0° to 70° 2θ range with a step size of 0.02 and scan speed of $3^\circ/\text{min}$. The observed peaks revealed that the obtained particles are face centred cubic with as average a crystalline size of 26.3nm. The prominent XRD diffraction peaks are indexed to 36.7,45.3, 47.6,52.3 and 65.7 and the corresponding planes are (111),(220), (200),(311),(222) respectively. The average crystalline size 'D' of the as obtained NiO nanoparticles were estimated by Debye-Scherrer equation

$$D=0.89 \lambda/\beta \cos \theta$$

Where λ is the wavelength of the incident beam ($\lambda = 1.5406 \text{ \AA}$) and β is the full width at half maximum and θ is the Bragg's diffraction angle. For face centred cubic crystal structure of NiO, the inter planar spacing 'd' is calculated using the expression

$$D_{hkl} = a / \sqrt{h^2+k^2+l^2}$$

Where 'a' represents the lattice parameter constant and h, k, l are the Miller indices. The evaluated average crystallite size of the nanoparticle was 26.132 nm using high intensity Bragg peak of (200). The Williamson Hall Plot for NiO using XRD calcination is shown in Fig 5.

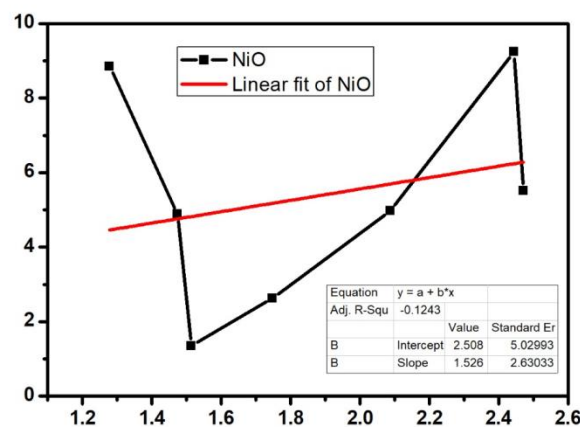


Fig 5. Williamson Hall Plot for as prepared NiO nanoparticles

The crystal defect may cause peak broadening which induced strain in grown lattice. W-H plot method was utilised to investigate the variation in strain and crystallite size as a function of 2θ to deconvolute size induced and strain induced broadening [23-24]. The W-H method does not varies as $1/\cos\theta$ as in the Scherrer equation but instead it varies with $\tan\theta$. The combination of peak broadening due to Particle size and lattice strain is given as the total peak broadening can be written as

$$\beta_{hkl} = \beta_D + \beta_s$$

Strain induced broadening is given as

$$B_s = 4 e \tan\theta$$

By putting values of β_D and β_s in the above equation

$$\beta_{hkl} = [k\lambda/D] + 4 e \sin\theta$$

For W-H analysis, plot is drawn between $4 \sin\theta$ and $\beta \cos\theta$ as shown in the Figure. By linear fitting the data, the value of slope and y-intercept is used to calculate strain and size for NiO sample was found to be 23.46

nm in the W-H plot. Hence the sizes of NiO nanocrystals obtained from W - H analysis are well correlated with sizes estimated using Scherrer's formula.

3.2 FTIR analysis:

Fig 6. represents the FTIR spectrum of as prepared NiO nanoparticles calcined at 400° c for 3 hours. The bands due to the Oxide structure are clearly seen in the region between 400 and 850 cm^{-1} [25]. The two peaks at 3400 cm^{-1} and 1650 cm^{-1} are attributed to the surface adsorbed water and hydroxyl groups [26]. The peak at 3640 cm^{-1} corresponded to H- bonded phenols and 3005 and 2934 cm^{-1} , suggesting OH and H bonded carboxylic groups [27].

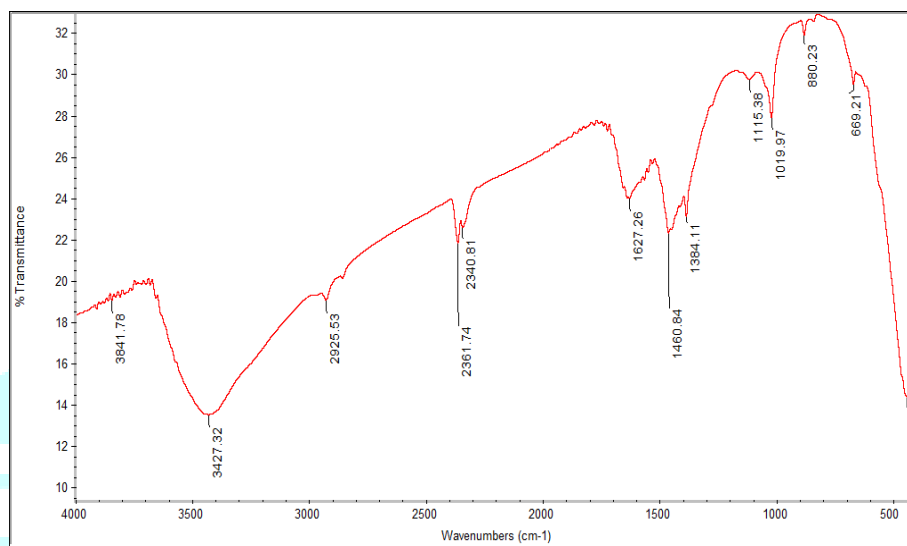


Fig 6. FTIR spectrum of as prepared NiO nanoparticles.

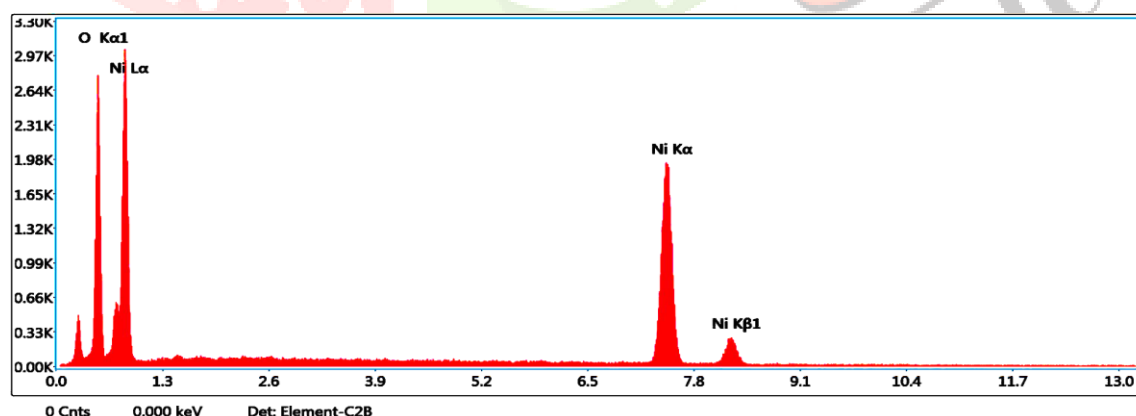
Moreover, the peaks between 1000 and 400 cm^{-1} corresponds to the structural vibrations of Ni-OH and Ni-O-Ni interactions. The broad absorption band centred at 1725 cm^{-1} is attributing to bending mode of H-O-H. The significant absorption peak at 450 cm^{-1} is due to the CO-O stretching vibration mode. The absorption peak at 2925.53 cm^{-1} is due to the $-\text{CH}_2$ stretching vibrations. The absorption peaks at 2925.53 cm^{-1} is also due to the $-\text{CH}_2$ stretching vibrations. The absorption bands at 470 cm^{-1} and 522 cm^{-1} are assigned to the Ni-O vibration band, but absorption band at 619 cm^{-1} is attributed to the Ni-O-H stretching bond. This confirms the formation of pure NiO nanoparticles. Additionally the broad absorption band at 3427.32 cm^{-1} and a weak band at 1627.26 cm^{-1} are assigned to OH stretching and bending modes of water respectively [28]. The wide absorption band around 1381 cm^{-1} is assigned to CO_3^{2-} ions. The peak at 1033 cm^{-1} corresponds to stretching and bending vibrations of the inter calated c-o species and the bands at 2924 cm^{-1} and 2854 cm^{-1} are attributed to CH_2 vibrations. The peaks observed at 416 cm^{-1} corresponds to Ni-O particles stretching mode [29-30]. The detailed functional groups and the assignments of NiO nanoparticles is tabulated in Table 1.

Table 1. Frequency assignments for as prepared NiO nanoparticles

WAVE NUMBER (cm ⁻¹)	ASSIGNMENT
3427.32	OH broader band group
2925.53	C-H stretch at sharp band
2361.74	C ≡ C
1627.26	C=C stretch bond
1384.11	NO groups
1115.38	C = H group

3.3 EDAX Analysis:

Fig.7 shows the typical EDAX pattern of as prepared NiO nanoparticles. The quantitative composition analysis of NiO nanoparticles was carried out using Energy Dispersive X-Ray Spectroscopy measurement. The concentration of elements Ni and O varies periodically along the atom size being accompanied with maxima of Ni along 49% and O along 51% as shown in Table 2,

**Fig 7. EDAX spectrum of as prepared NiO nanoparticle**

Element	Weight %	Atomic %	Error %	Kratio
Ok	22.1	51.0	7.4	0.1153
Nik	77.9	49.0	2.2	0.7360

Table 2. EDAX data of as prepared NiO nanoparticles

There is no evidence of impurity in the composition. Fine particles tends to form agglomerated and fine spherical shape of powered particles are frequently seen on the surface of powders from SEM analysis. The

surface concentration of oxygen looks like coarse islands the height is also considered. The Ni atom in the oxidation state are concentration in the oxide from is the metallic state as shown in the SEM image [31-32].

3.4 SEM studies:

The NiO nanoparticles in the SEM image is shown in Fig 8. depicts a spherical nanoparticle structure. The size of the NiO nanoparticle ranges between 20 and 60 nm. Moreover, a few of them were slightly agglomerated which is due to the range volume of heat carried out during the synthesis procedure. However the small sized particles were highly reactive due to sharp edges, which contain a high surface to volume ratio and less cohesive energy compared with bulk materials [33-34]. The instrumental parameters, accelerating voltage spot size and magnification and working distances are marked on the SEM image as shown in the Fig 7. The results indicate that monodispersive and highly crystalline NiO nanoparticles are obtained, so we can infer that the as prepared NiO nanoparticle are in the nanometer range. The average diameter of the particle observed from SEM analysis 94 nm which is larger than the diameter predicted from the X-ray broadening.

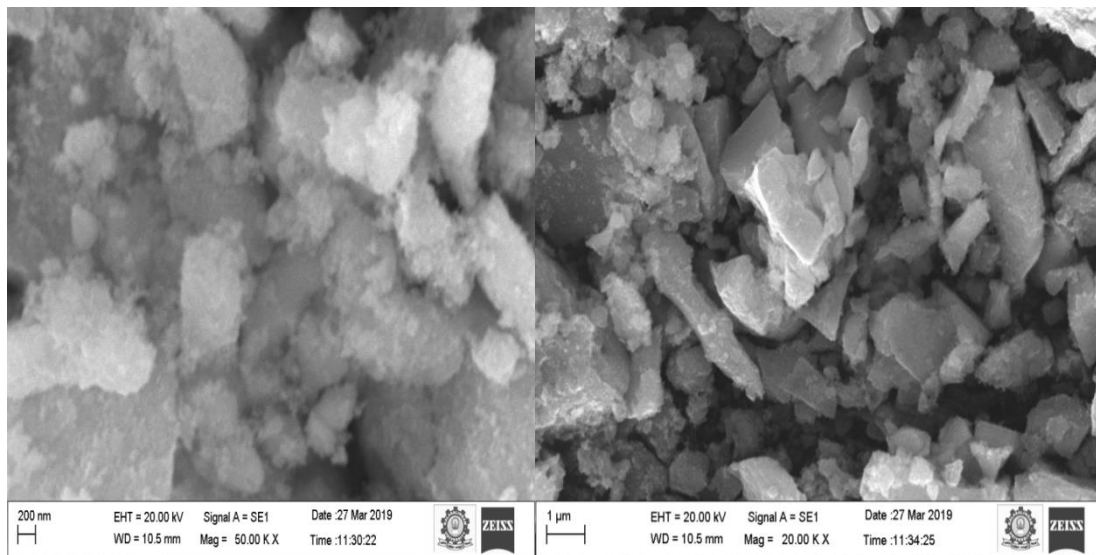


Fig 7 SEM Images at 200nm, 1μm of as prepared NiO nanoparticles

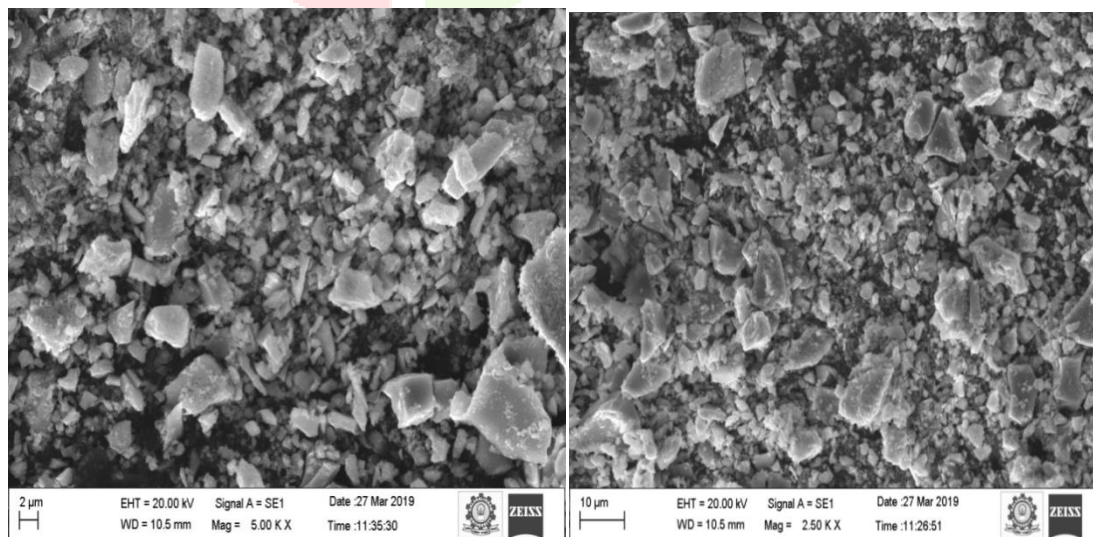


Fig 8 SEM Images at 2μm,10μm of as prepared NiO nanoparticles

Conclusions

The nanoparticles of NiO have been successfully synthesized by a one step solvothermal synthesis method at room temperature XRD analysis shows the sample prepared are in cubical phase. The broad peak of XRD analysis indicates the nano crystalline behaviour of the particles. The FTIR analysis ascertains all the functional groups in NiO nanoparticles. EDAX analysis confirms the presence of Nickel and Oxygen in the sample. SEM analysis visualise that the NiO nanoparticle are spherical in size with a dimension ranging from 85-95 nm.

Acknowledgements

The authors would like to thank Rev. Dr. S. Mariadass S.J, the principal of St. Xavier's College, Palayamkottai and Rev. Dr. Alphones Manickam S.J, the secretary of St. Xavier's College, Palayamkottai for their constant support and encouragement.

Reference

1. N. R. Jana, Y. F. Chen and X.G. Peng, Size-and Shape-Controlled Magnetic Oxide nanocrystals via a simple and general approach, *Chem. Mater.*,16,2004, 3931-3935.
2. W. Wei, X.Jiang, L.Lu, X. Yang and X. Wang, Study on the catalytic effect of NiO nanoparticles on the thermal decomposition of TEGDN/NC propellant, *J. Hazard. Mater.*, 168,2009,838-842.3.
3. N. R. E. Radwan, M. S. El-Shall and M. A. Hassan, Synthesis and characterization of nanoparticle Co₃O₄, CuO and NiO catalysts prepared by physical and chemical methods to minimize air pollution, *Appl. Catal. A. Gen.* 331, 2007,8-18.
4. X.W. Lou, D. Deng, J.Y. Lee and L.A. Archer, Thermal formation of mesoporous single-crystal Co₃O₄ nano-needles and their lithium storage properties, *J. Mater. Chem.*, 18, 2008, 4397-4401. DOI 10.1039/B810093D
5. X.W. Lou, D. Deng, J.Y. Lee, J. Feng and L.A. Archer, Self-Supported Formation of Needlelike Co₃O₄Nanotubes and Their Application as Lithium-Ion Battery Electrodes *Adv. Mater.*, 20, 2008, 258 -262. DOI 10.1002/adma.200702412
6. I. Hotovy, J. Huran and L. Spiess, Preparation and characterization of NiO thin films for gas sensor application, *Vacuum* 58, 2000, 300-307.
7. Z.Z. Lin, F.L. Jiang, L. Chen, C.Y. Yue, D.Q. Yuan, A.J. Lan and M.C. Hong, A Highly Symmetric Porous Framework with Multi-intersecting Open Channels, *Cryst. Growth Des.*, 7, 2007, 1712-1715. DOI 10.1021/cg060732o
8. Q. Zhao, Z. Zhang, T. Dong and Y. Xie, Facile Synthesis and Catalytic Property of Porous Tin Dioxide Nanostructures, *J. Phys. Chem. B*, 110, 2006, 15152- 15156, DOI 10.1021/jp0620522
9. M. Yoshio, Y. Todorov, k. Yamato, H. Noguchi, J. Itoh, M. Okada and T. Mouri, Preparation of Li_yMnxNi_{1-x}O₂ as a cathode for lithium-ion batteries, *J. Power sources* 74, 1998,46-53.

10. G.A. Seisenbaeva, M.P. Moloney, R. Tekoriure, A.H. Dessources, J.M. Nedelec, Y. K. Gun'Ko, Vadim G. Kessler, Biomimetic Synthesis of Hierarchically Porous Nanostructured Metal Oxide Microparticles Potential Scaffolds for Drug Delivery and Catalysis, *Langmuir* 26, 2010, 9809- 9817. DOI 10.1021/la1000683_
11. A. Chrissanthopoulos, S. Baskoutas, N. Bouropoulos, V. Dracopoulos, P. Pouloupoulos, S. N. Yannopoulos, Synthesis and characterization of ZnO/NiO p n heterojunctions: ZnO nanorods grown on NIO thin film by thermal evaporation, *Photon, Nanostructures*, 9, 2011, 132-139.
12. T. Stimpfling, F. Leroux, Supercapacitor-Type Behavior of Carbon Composite and Replica Obtained from Hybrid Layered Double Hydroxide Active Container, *Chem. Mater.*, 22, 2010, 974- 987, DOI 10.1021/cm901860y
13. F. Davar, Z. Fereshteh, M.S. Niasari, Nanoparticles Ni and NiO: Synthesis, characterization and magnetic properties, *J. Alloys and Compounds*, 476, 2009, 797-801, DOI 10.1016/j.jallcom.2008.09.121
14. M.W. Zhu, Z.J. Wang, Y.N. Chen, Z.D. Zhang, Microwave processing of conductive lanthanum nickel oxide films in separated microwave magnetic field, *Surface & Coatings Tech.* 216, 2013, 139- 144, DOI 10.1016/j.surfcoat.2012.11.041.
15. Thema, F.T.; Manikandan, E.; Gurib-Fakim, A.; Maaza, M. Single phase Bunsenite NiO nanoparticles green synthesis by *Agathosma betulina* natural extract. *Journal of Alloys and Compounds* **2016**, 657, 655-661, <https://doi.org/10.1016/j.jallcom.2015.09.227>.
16. Taghizadeh, F. The Study of Structural and Magnetic Properties of NiO Nanoparticles. *Optics and Photonics Journal* **2016**, 06,164-169, <https://doi.org/10.4236/opj.2016.68B027>.
17. Olaitan, A.D.; Reyes, K.A.; Barnes, L.F.; Yount, J.R.; Ward, S.; Hamilton, H.S.C.; King, K.E.; Van Leeuwen, C.J.; Stepherson, J.R.; Vargas, T.K.; Kirkconnell, M.P.; Molek, K.S. Transition metal oxide nanoparticles as surfaces for surface-assisted laser desorption/ionization mass spectrometry of asphaltenes. *Petroleum Science and Technology* **2017**, 35, 1917-1924, <https://doi.org/10.1080/10916466.2017.1370476>.
18. Pomerantz, A.E.; Wu, Q.; Mullins, O.C.; Zare, R.N. Laser-Based Mass Spectrometric Assessment of Asphaltene Molecular Weight, Molecular Architecture, and Nanoaggregate Number. *Energy & Fuels* **2015**, 29, 2833-2842, <https://doi.org/10.1021/ef5020764>.
19. Hou, Y.; Kondoh, H.; Ohta, T.; Gao, S. Size- controlled synthesis of nickel nanoparticles. *Applied Surface Science* **2005**, 241, 218-222, <https://doi.org/10.1016/j.apsusc.2004.09.045>.
20. Qi, X.; Su, G.; Bo, G.; Cao, L.; Liu, W. Synthesis of NiO and NiO/TiO₂ films with electrochromic and photocatalytic activities. *Surface and Coatings Technology* **2015**, 272, 79-85, <https://doi.org/10.1016/j.surfcoat.2015.04.020>.

21. Cordente, N.; Amiens, C.; Chaudret, B.; Respaud, M.; Senocq, F.; Casanove, M.J. Chemisorption on nickel nanoparticles of various shapes: Influence on magnetism. *Journal of Applied Physics* **2003**, *94*, 6358-6365, <https://doi.org/10.1063/1.1621081>.
22. Gong, J.; Wang, L.L.; Liu, Y.; Yang, J.H.; Zong, Z.G. Structural and magnetic properties of hcp and fcc Ni nanoparticles. *Journal of Alloys and Compounds* **2008**, *457*, 6-9, <https://doi.org/10.1016/j.jallcom.2007.02.124>.
23. A.K.Zak, W.H.A Majid, M.E. Abirashmi R. Youse, X-ray analysis of ZnO nanoparticles by Williamson Hall method and size strainplot methods Vol 13, (2011), <https://doi.org/10.1016/solidstate-sciences> 2010.1024.
24. P.B.S. Thomas, Estimation of lattice strain in ZnO Nanoparticles. X-ray peak profile analysis (2014), pp 123- 134, <https://doi.org/10.1007/40094014-0141-9>.
25. D.Khushalini, O.Dag, G.A O Zin and A Koperman *J.Mater. chem.* **9** (1999) 491-1500.
26. G.J, Li and S.Kawi *Talanta* **45** (1998)759-766.
27. Saleem ,S ; B. Ahmed M.S khan; AL-Shaerim; Mussarat . J, Inhibition of growth and biofilm formation of clinical bacterial isolates by NiO nanoparticles synthesized from Eucalyptus flobulus plants, *Microb. Patbogen* **2017**, *111*, 375-387.
28. L. Wu, Y. Wu, H. Wei *Materials letters* **58** (2004) 2700-2703.
29. J. Li, R. Yan, B. Xian, D.T. Liang D.H. Lee, *Energy Fuels* **22**(1) 2008 16-23
30. X. Song, L. Geo, J. *American ceramic Society* **91** (2008) 3465-3468.
31. Hill Aw, Shears AL, Hibbit KG, Increased Antibacterial activity Against E. Coli in Bovine serum after the induction of endotoxin tolerance, *Am. Soc. Micro* **1976**, *14*-257-65
32. Baskoutass, Terziz HF, size dependant band gap of colloidal quantum dots, *AIP J. Ap. Physics*, **2006**, *99*-013708
33. Bashir A.K.H, Razana Mabandry L.C, Nivanya A.C, K. Kariyasu, SabanW; Mohamed A.E.A Bio Synthesis of NiO nanoparticles for photo degradation of free cyanide solutions under ultra violet light *J. Phy. Chem. Solids* **2019**, *134*, 133-140.
34. Mallikarjuna k, Kim H, Synthesis and characterization of highly active Cu Ad Bimetallic nanostructures colloid. *Sufs. A.* **2017**, *535*, 194-200.